

CrossMark
click for updatesCite this: *RSC Adv.*, 2016, 6, 76874Received 12th May 2016
Accepted 1st August 2016

DOI: 10.1039/c6ra12334a

www.rsc.org/advances

Acidithiobacillus ferrooxidans improved H₂S gas sensing properties of tubular hydroxyapatite at room temperature

Yanni Tan,^a Huixia Li,^a Yong Liu,^{*a} Jianping Xie,^b Jia He^b and Jun Pan^a

A novel H₂S gas sensing composite based on tubular hydroxyapatite (HAp) and *Acidithiobacillus ferrooxidans* (*At.f*) was prepared, and the gas sensing properties of pure HAp and the composite to H₂S were studied. The microstructures, crystalline phases and chemical groups of the composites were characterized by SEM, TEM, XRD, and FTIR. Results show that jarosite was formed during the cultivation of *At.f*. Compared to pure HAp, the composite exhibited a more excellent response to H₂S. With the increase of the amount of *Acidithiobacillus ferrooxidans* added, the sensitivity of the composite to H₂S increased. The composite showed a highest sensitivity of 76% to H₂S at 2000 ppm, which is 2.5 times that of pure HAp. The probable sensing mechanisms of the composite to H₂S were proposed. Other than the *At.f*, the structure and the chemical groups of jarosite are also beneficial for H₂S gas sensing.

1. Introduction

Hydrogen sulfide (H₂S) is a toxic, inflammable, corrosive, and malodorous acid gas, produced in coal mines, petroleum fields, sewage, and natural gas production. It is extremely harmful to both the human body and the environment. According to the safety standards established by the American Conference of Government Industrial Hygienists (ACGIH), the threshold limit value (TLV) defined for H₂S is 10 ppm for 8 h.^{1,2} Even at a low concentration, H₂S exerts a severe effect on the nervous system, and may cause death at a concentration higher than 250 ppm. Therefore, there is an urgent demand for gas sensors with a low cost and high sensitivity for the detection and monitoring of H₂S.

Many efforts have been made to prepare H₂S gas sensors. The most studied materials are metal oxides, such as WO₃, SnO₂, Fe₂O₃, TiO₂, ZnO and In₂O₃, as well as the composites

based on them, such as PPy/WO₃,³ CuO/ZnO,⁴ In₂O₃/ZnO,⁵ Fe-doped SnO₂,² Cu-doped SnO₂,⁶ and Pt-doped Fe₂O₃.¹ Usually, the composites exhibit better gas sensing performance than single oxides. However, most of the H₂S gas sensing materials reported need to be operated at elevated temperatures. For instance, the operation temperatures of CuO/ZnO, TiO₂, Fe₂O₃ sensors are 300–500 °C,⁴ 225–325 °C,⁷ and 200–600 °C,⁸ respectively. Some materials have been studied as gas sensors that can be operated at room temperature, such as SnO₂/CuO,⁹ Fe-doped SnO₂,² and PPy/WO₃ nanocomposite films.³ PPy/WO₃ has good sensitivity, reversibility and long-term stability at room temperature, but it has low sensitivity at a low concentration of H₂S (<100 ppm).³

Hydroxyapatite (HAp) exhibits peculiar properties, such as surface P–OH bond which interacts with the gas molecules to be detected, highly porous structure and capability to exchange ions, so HAp has attracted more and more attentions in gas sensor filed. The authors have reported the sensing properties of tubular hydroxyapatite and composites.^{10–13} It was found that tubular hydroxyapatite exhibits high sensitivity, quick response and recovery time, excellent reproducibility and selectivity to ammonia gas at room temperature.¹⁰ Pure tubular HAp also showed response to H₂S, but the sensitivity is not high.

Acidithiobacillus ferrooxidans (*At.f*), a Gram-negative bacterium, is a dominant organism in biohydrometallurgy in the process of ore bioleaching, and has been utilized in the processes of desulphurization of sour gases and coal.¹⁴ These bacteria can obtain energy through the electrons released as a consequence of the oxidation process of Fe²⁺ to Fe³⁺ and elemental sulfur in acidic solution. During the oxidation process, *At.f* acts as a catalyst of the formation of jarosite.¹⁵ Jarosite has been found to be an effective photocatalytic material.^{15,16} However, the gas sensing properties of *At.f* or jarosite have not been reported so far.

In this work, *At.f* bacteria was mixed with HAp to prepare a novel gas sensing material, in order to improve the sensitivity of HAp to H₂S.

^aState Key Laboratory of Powder Metallurgy, Central South University, Changsha 410083, PR China. E-mail: yonliu@csu.edu.cn

^bSchool of Minerals Processing and Bioengineering, Central South University, Changsha 410083, PR China

2. Materials and methods

HAp was fabricated using a cation exchange membrane assisted electrochemical deposition method, as reported in our previous work.¹⁰ *At.f* was conventionally cultivated using 9 K medium with a pH value of 2. The inoculation size was 5 ml strain per 100 ml medium. The flask was incubated on a rotary shaker for 8 h at 30 °C. The alive bacteria were collected and washed by the centrifugation method. *At.f* collected from different amounts of medium (100 ml, 200 ml and 500 ml) were re-dispersed in 50 ml water using a centrifugal tube, and were mixed with 0.21 g HAp respectively by shaking for 4 h. The composites were denoted as 1*At.f*/HAp, 2*At.f*/HAp and 5*At.f*/HAp respectively. Finally, the composite was centrifuged, washed and dried in vacuum at 50 °C. The bacteria in the composite should be dead.

The morphology was investigated by using field emission scanning electron microscope (FESEM; NOVA NANOSEM, USA), and field emission transmission electron microscope (FETEM; JEOL JEM-2100F, Japan). The crystalline phase and chemical groups were tested by X-ray Diffraction (XRD, D/ruax 2550PC) and Fourier Transform Infrared Spectroscopy (FTIR, Thermo/USA Nicolet Nexus 670FTIR).

Gas sensing properties were measured by a Chemical gas sensor-8 (CGS-8, Beijing Elite Tech Co., Ltd, China) intelligent gas sensing analysis system. The details of the detection method has been reported before.¹³ Simply, HAp and *At.f*/HAp composites were coated on a ceramic tube with 4 Au electrodes to make the sensor. The gas sensing properties were measured in a 1 l glass bottle. Firstly, the bottle was vacuumed, and injected with a certain amount of H₂S. After the H₂S diffused absolutely, the air was allowed to enter and mix homogeneously. Secondly, the sensor was put into the bottle immediately, and the electric resistance of the sensor changed rapidly. When the resistance reached a stable level, the sensor was taken out, and the resistance came back to the initial value. The sensitivity of the sensors was denoted using the equation: $S = (R_a - R_g)/R_a \times 100\%$, in which R_a and R_g were the resistance of the sensors in dry air and target gas respectively.

3. Results and discussion

The microstructural observations (Fig. 1(a–c)) show that *At.f* is rod-like, 100–200 nm wide and 0.5–1 μm long, and is apt to forming clusters. HAp exhibits tubular morphology, with a diameter of 2.5–5 μm, and a length of 5–20 μm. The tubular is made up of clusters of nanorods with a diameter of 10–20 nm and a length of about 100 nm (Fig. 1(d and e)). *At.f* and HAp were mixed physically (Fig. 1(f)).

From the XRD patterns of the *At.f* (Fig. 2), it can be seen that the crystalline phase in *At.f* is jarosite (KFe₃(SO₄)₂(OH)₆, PDF 22-0827). The formation process and mechanism of jarosite has been reported else where.^{14,17} Simply, during the culture of *At.f*, a series of chemical reactions occur, including the oxidation of ferrous iron, hydrolysis of ferric iron, and finally jarosite precipitation.¹⁷ The following is the formula for jarosite precipitation:

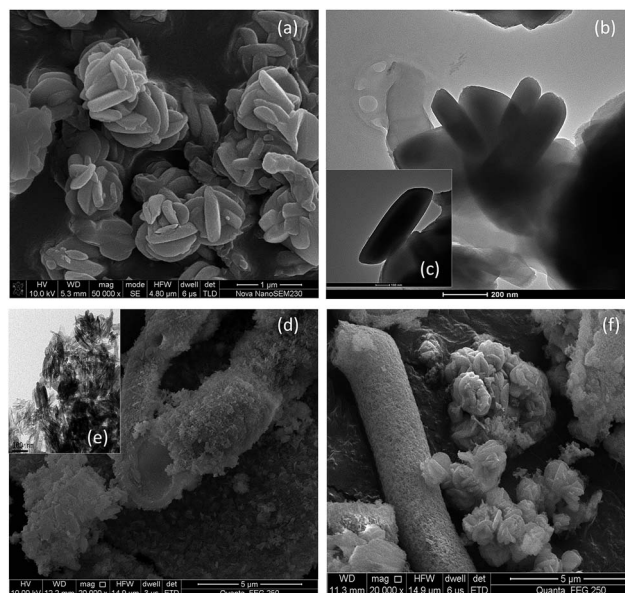


Fig. 1 Microstructures of *At.f* (a–c), HAp (d and e) and *At.f*/HAp composite (f).



The XRD patterns of *At.f*/HAp composite contain the characteristic peaks of HAp and jarosite. Fig. 3 shows the spectra of *At.f* and *At.f*/HAp composite. For *At.f*, the specific adsorption bands are observed at 1643 and 1543 cm⁻¹, which correspond to amide I: C=O vibrations of different protein structures and amide II: N–H and C–N vibrations of the peptide bond in different protein conformations. There are several peaks of jarosite. The intense absorption observed at 3389 and 1007 cm⁻¹ can be attributed to O–H stretching and deformation. The absorption bands at 1198 and 1086 cm⁻¹ are due to the ν₃ (doublet) vibrations of SO₄²⁻. The absorption at 631 cm⁻¹ can be attributed to the ν₄ vibration mode of SO₄²⁻. The bands observed at 512 and 475 cm⁻¹ are attributed to vibrations of

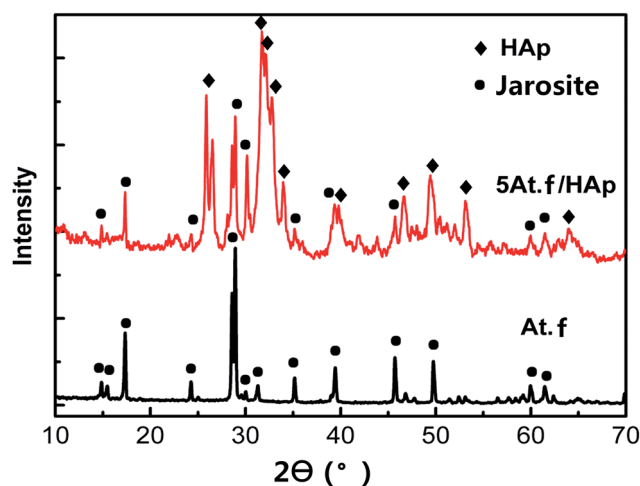


Fig. 2 XRD patterns of *At.f* and 5*At.f*/HAp composite.

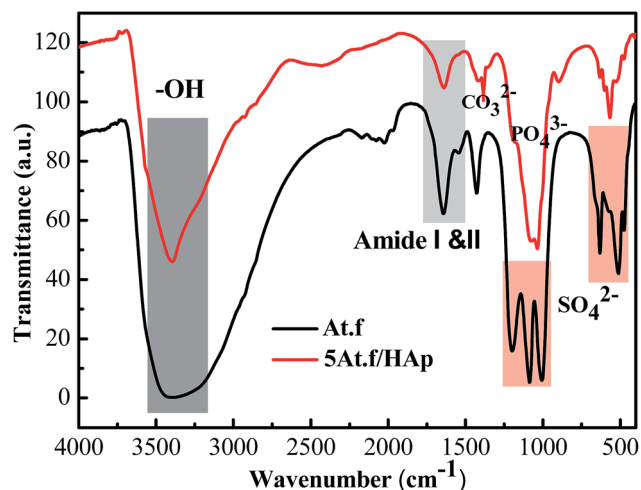


Fig. 3 FTIR spectra of *At.f* and *At.f*/HAp composite.

FeO₆ coordination octahedra.¹⁸ For *At.f*/HAp composite, besides the adsorption bands of *At.f*, there are the characteristic peaks at 567, 1036, and 1079 cm⁻¹, corresponding to ν_4 PO₄³⁻ bending vibration mode (567 cm⁻¹), and ν_3 PO₄³⁻ stretching vibration mode (1036, 1079 cm⁻¹) respectively. The band at 1384 cm⁻¹ may correspond to ν_3 asymmetric stretch vibration mode of CO₃²⁻ due to the reaction between OH of HAp and CO₂ in the air.

From the response–recovery curves (Fig. 4(a)), it can be seen that when the HAp and the *At.f*/HAp composite sensors are exposed to H₂S atmosphere, the resistance decreases and finally reaches a minimum value. When the sensors are taken out, the resistance recovers to the initial level gradually. For pure HAp, the sensitivity to H₂S is very low. For example, the sensitivity at 100 ppm and 2000 ppm are 18.4% and 31.2% respectively. Besides, with the increase of H₂S concentration, the sensitivity of HAp sensor increases a little. The response/recovery time is very short, and the smooth curve indicates good stability.

Compared to pure HAp, the H₂S sensing properties of composites are improved significantly. With the increase of *At.f* in composites, the sensitivity is improved to a large degree. For 1*At.f*/HAp, the sensitivity at concentrations below 400 ppm increases little, but at high concentrations above 600 ppm, the sensitivity improves by about 35%. The sensitivity of 2*At.f*/HAp in ranges of 100–1000 ppm improves by 35%, and by 67% at concentrations of 600 ppm and 1000 ppm. The sensitivity of 2*At.f*/HAp is two times that of pure HAp at 2000 ppm. The sensor based on 5*At.f*/HAp exhibits the highest sensitivity, reaching 75% at 2000 ppm. In ranges of 100–600 ppm, the sensitivity increases 100% compared to pure HAp, and at high concentrations above 1000 ppm, the sensitivity improves by about 135–150%. The response time is short and stable. However, the recovery time of 5*At.f*/HAp is longer than the other sensors and not stable enough.

From the curves of the sensitivity vs. H₂S concentration (Fig. 4(b)), it is found that at low concentrations (100–1000 ppm for 5*At.f*/HAp and 100–600 ppm for others), the sensitivity has a linear relationship with the concentration of H₂S, while at high concentrations (above 1000 ppm for 5*At.f*/HAp and 600 ppm for others), the sensitivity increases a little and tends to be saturated.

Since the 5*At.f*/HAp composite exhibits the highest sensitivity to H₂S, the sensing properties of 5*At.f*/HAp at H₂S concentrations lower than 100 ppm was further studied. Fig. 5 shows the linear ranges of 5*At.f*/HAp composite to H₂S. It can be concluded that the H₂S sensing properties of *At.f*/HAp at low concentrations are more stable than that at high concentrations. The response/recovery time at 20, 40, 80, 100 ppm of H₂S (Fig. 5(a)) are about 60 s, which is much shorter than that at high concentrations. Besides, the response sensitivity linearly depends on the increase of H₂S concentration from 20 ppm to 100 ppm. The broken line was fitted into a linear equation with a slope of 0.33, and correlation coefficient (R^2) is 0.98, indicating the data points correspond well to the regression equation. The degree of linearity between the sensitivity and H₂S

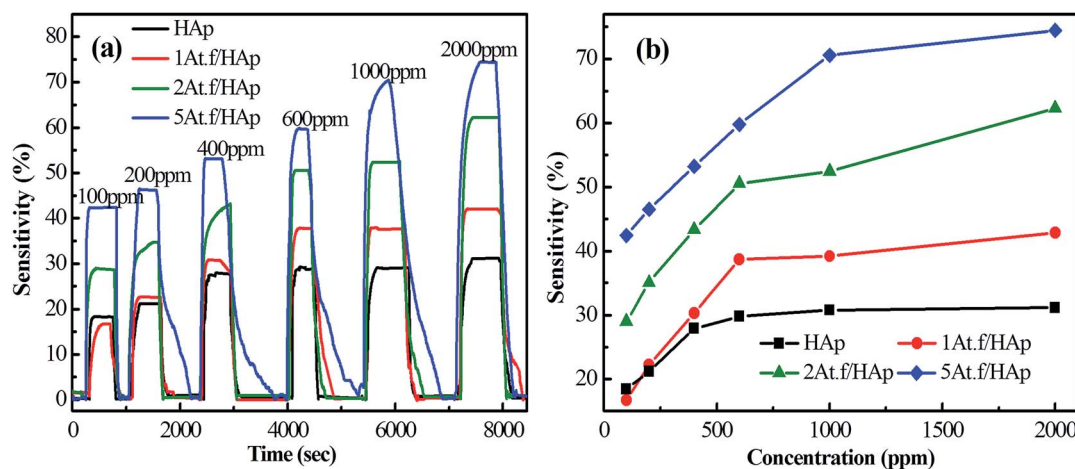


Fig. 4 Response–recovery curves (a) and gas sensitivities curves (b) of HAp, 1*At.f*/HAp, 2*At.f*/HAp and 5*At.f*/HAp composites to H₂S at different concentrations in range of 100–2000 ppm at room temperature.

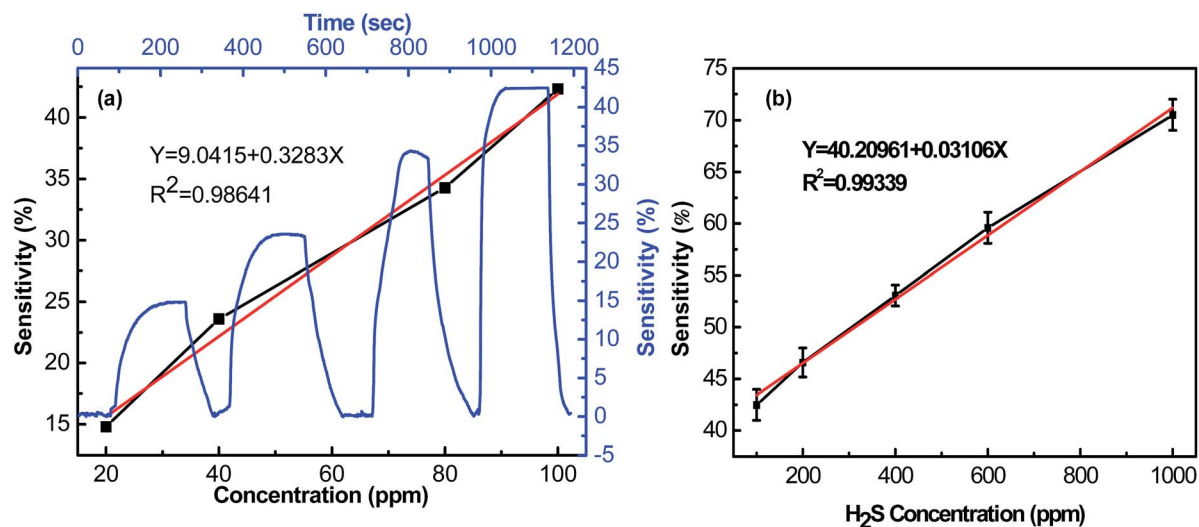


Fig. 5 Response–recovery curves and gas sensitivity curves of 5*At.f*/HAp composites to H₂S at different concentrations in range of 20–100 ppm (a), linear relations between the gas sensitivities of 5*At.f*/HAp to H₂S at concentrations in range of 100–1000 ppm at room temperature (b).

concentration is very high. At concentrations from 100 ppm to 1000 ppm (Fig. 5(b)), the sensitivity of 5*At.f*/HAp to H₂S also increases linearly with the increase of H₂S concentrations. But the slope is 0.031, much smaller than that in ranges of 20–100 ppm, showing that the sensitivity linearly increases more quickly with the increase of concentrations from 20 ppm to 100 ppm.

The sensing properties as well as sensing mechanisms of tubular HAp to NH₃ and some volatile organic compounds (VOCs) have been discussed in precious work.¹⁰ As reported, the preferential growth along (002) orientation (*c*-axis), poor crystallinity, high surface-to-volume ratio, mesoporous feature and tubular structure provide the tubular HAp abundant adsorption sites for the target gases to be sensed. A small amount of H₂S was adsorbed by hydrogen bonding with H₂O that are absorbed on the surface of HAp. The low sensitivity of pure HAp to H₂S indicates the limited adsorption of H₂S. But the sensitivity of *At.f*/HAp composites to H₂S improved significantly. Therefore, the chemical components and structural characteristics of *At.f* may be helpful for the adsorption of H₂S. The cell wall of *At.f* is

composed of various proteins and polysaccharides, making the surface of *At.f* enriched of chemical active groups such as mercapto-group, hydroxyl and carboxyl. This active groups can easily react with gas molecules resulting in the strong adsorption capacity of the composites. Besides, due to the existence of

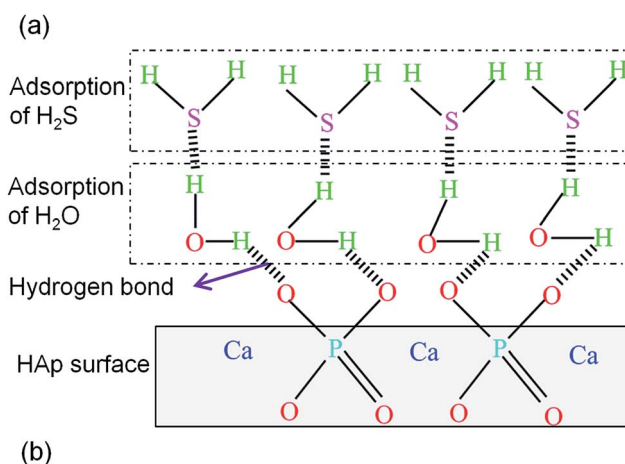


Fig. 7 Gas sensing mechanism diagram of *At.f*/HAp composite to H₂S: H₂S gas absorbed on the surface of HAp (a); H₂S gas molecules sensed on *At.f*/HAp composite (b).

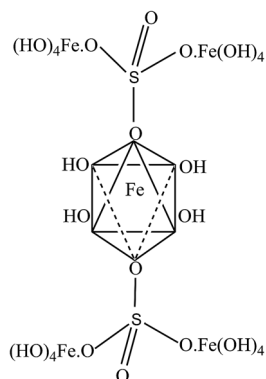


Fig. 6 Structure of jarosite: single unit.

vapor, H₂S may be dissociated to HS⁻ and H⁺. Since proton was acknowledged to be the charge carrier of HAp, the dissociation of H₂S increases the density of proton in HAp, so the resistance of the HAp decreases when exposing to H₂S.

Another reason for the improvement of the sensitivity is attributed to jarosite that is formed during the cultivation of *At.f.* Recently, jarosite has been used to enhance the photocatalytic activity of TiO₂,¹⁶ and as a heterogeneous Fenton catalyst for dye decolorization,¹⁹ as well as the photocatalyst for degradation of methyl orange (MO) azo dye.¹⁵ The structure of jarosite (Fig. 6) is made up of layers of tilted Fe(OH)₄O₂ octahedra, joining layers of combined sulphate tetrahedral and alkali coordination icosahedra,²⁰ which may be beneficial for the adsorption of H₂S. Fe³⁺ is coordinated by four OH⁻ groups and two oxygen atoms from two separate SO₄²⁻ groups. As a catalyst, hydroxyl radical in jarosite plays the predominant role in MO degradation.¹⁵ The enhancing effect of sensing properties of HAp to H₂S may also be due to the multiple OH⁻ groups in jarosite, which can provide the adsorption sites for H₂S. In addition, it was shown that the catalysts containing the oxide and sulfate compounds of iron provide the selective oxidation of hydrogen sulfide to sulfur.²¹ So, Fe³⁺ and SO₄²⁻ in jarosite may also be beneficial for the sensitivity to H₂S. Based on the above discussion, a simple mechanism diagram was shown in Fig. 7.

4. Conclusions

A novel sensing material composing of *Acidithiobacillus ferrooxidans* (*At.f.*) and tubular hydroxyapatite for H₂S was developed. The sensing properties were significantly improved by *At.f.* The sensitivity of 5*At.f.*/HAp was 2.5 times of pure HAp. The response/recovery time of the composite is short and stable. The sensing mechanism of the composites to H₂S was proposed to be closely associated with the structure and the chemical composition of *At.f.* The layered structure of jarosite, as well as the OH⁻, Fe³⁺ and SO₄²⁻ groups in jarosite plays an important role for the enhancement of the sensing properties to H₂S. The *At.f.*/HAp composites shows promising application to sense H₂S gas.

Acknowledgements

This research was financially supported by the National Natural Science Foundation of China (No. 51272289), State Key Laboratory of Powder Metallurgy, CSU and the Fundamental

Research Funds for the Central Universities of Central South University (2015zzts180).

Notes and references

- 1 Y. Wang, S. Wang, Y. Zhao, B. Zhu, F. Kong, D. Wang, S. Wu, W. Huang and S. Zhang, *Sens. Actuators, B*, 2007, **125**, 79–84.
- 2 M. V. Vaishampayan, R. G. Deshmukh, P. Walke and I. Mulla, *Mater. Chem. Phys.*, 2008, **109**, 230–234.
- 3 P.-G. Su and Y.-T. Peng, *Sens. Actuators, B*, 2014, **193**, 637–643.
- 4 J. Kim, W. Kim and K. Yong, *J. Phys. Chem. C*, 2012, **116**, 15682–15691.
- 5 W. Zang, Y. Nie, D. Zhu, P. Deng, L. Xing and X. Xue, *J. Phys. Chem. C*, 2014, **118**, 9209–9216.
- 6 G. P. Shukla and M. C. Bhatnagar, *J. Mater. Sci. Eng. A*, 2014, **4**, 99–104.
- 7 G. Chaudhari, D. Bambole, A. Bodade and P. Padole, *J. Mater. Sci.*, 2006, **41**, 4860–4864.
- 8 Z. Zhang, H. Jiang, Z. Xing and X. Zhang, *Sens. Actuators, B*, 2004, **102**, 155–161.
- 9 L. Patil and D. Patil, *Sens. Actuators, B*, 2006, **120**, 316–323.
- 10 H. Li, Y. Liu, Y. Tan, L. Luo, Q. Zhang, K. Li and H. Tang, *New J. Chem.*, 2015, **39**, 3865–3874.
- 11 Q. Zhang, Y. Liu, H. Li, Y. Tan, L. Luo, J. Duan, K. Li and C. E. Banks, *Analyst*, 2015, **140**, 5235–5242.
- 12 H. Li, Y. Liu, L. Luo, Y. Tan, Q. Zhang and K. Li, *Mater. Sci. Eng., C*, 2016, **59**, 438–444.
- 13 L. Luo, Y. Liu, Y. Tan, H. Li, Q. Zhang and K. Li, *J. Cent. South Univ.*, 2016, **23**, 18–26.
- 14 J. Daoud and D. Karamanev, *Miner. Eng.*, 2006, **19**, 960–967.
- 15 Z. Xu, J. Liang and L. Zhou, *J. Alloys Compd.*, 2013, **546**, 112–118.
- 16 J. Xu, Z. Xu, M. Zhang, J. Xu, D. Fang and W. Ran, *Mater. Chem. Phys.*, 2015, **152**, 4–8.
- 17 S. I. Grishin, J. M. Bigham and O. H. Tuovinen, *Appl. Environ. Microbiol.*, 1988, **54**, 3101–3106.
- 18 J. Liu, B. Li, D. Zhong, L. Xia and G. Qiu, *J. Cent. South Univ. Technol.*, 2007, **14**, 623–628.
- 19 Z. Wang, D. Xiao, R. Liu, Y. Guo, X. Lou and J. Liu, *J. Adv. Oxid. Technol.*, 2014, **17**, 104–108.
- 20 G. Das, S. Acharya, S. Anand and R. Das, *Miner. Process. Extr. Metall. Rev.*, 1996, **16**, 185–210.
- 21 R. Terörde, P. Van den Brink, L. Visser, A. Van Dillen and J. Geus, *Catal. Today*, 1993, **17**, 217–224.